We are IntechOpen,
the world's leading publisher of
Open Access books
Built by scientists, for scientists

4,800
Open access books available

122,000
International authors and editors

135M
Downloads

Our authors are among the

154
Countries delivered to

TOP 1%
most cited scientists

12.2%
Contributors from top 500 universities

BOOK CITATION INDEX
CLARIVATE ANALYTICS
INDEXED

WEB OF SCIENCE™

Selection of our books indexed in the Book Citation Index
in Web of Science™ Core Collection (BKCI)

Interested in publishing with us?
Contact book.department@intechopen.com

Numbers displayed above are based on latest data collected.
For more information visit www.intechopen.com

Relaxor Behaviour in Ferroelectric Ceramics

A. Peláiz-Barranco, F. Calderón-Piñar,

O. García-Zaldívar and Y. González-Abreu

Additional information is available at the end of the chapter

1. Introduction

Ferroelectric materials are commonly characterized by high dielectric permittivity values [1]. Usually, for the well-known 'normal' ferroelectrics the temperature of the maximum real dielectric permittivity (T_m) corresponds to the ferroelectric-paraelectric (FE-PE) phase transition temperature (T_C) [2]. On the other hand, there are some kinds of ferroelectrics, so-called relaxor ferroelectrics, which have received special attention in the last years because of the observed intriguing and extraordinary dielectric properties [3-25], which remain not clearly understood nowadays. For instance, some remarkable characteristics of the dielectric response of relaxor materials can be summarized as follows: i- they are characterized by wide peaks in the temperature dependence of the dielectric permittivity, ii- the temperature of the corresponding maximum for the real (ε') and imaginary (ε'') component of the dielectric permittivity (T_m and $T_{\varepsilon''max}$, respectively) appears at different values, showing a frequency dependent behaviour, and iii- the Curie-Weiss law is not fulfilled for temperatures around T_m. So that, the temperature of the maximum real dielectric permittivity, which depends on the measurement frequency, cannot be associated with a FE-PE phase transition.

Lead zirconatetitanate (PZT) system is a typical ferroelectric perovskite showing 'normal' FE-PE phase transition [1]. Nevertheless, the partial substitution by different elements, such as lanthanum, contributes to enhance such relaxor characteristics [11-15]. In fact, for some lanthanum concentrations, the distortion of the crystalline lattice in the PZT system due to ions displacement could promote the formation of the so-called polar nanoregions (PNRs). Another interesting relaxor ferroelectric perovskite is known as PZN-PT-BT [16-19]. The $Pb(Zn_{1/3}Nb_{2/3})O_3$ ferroelectric material (PZN) belongs to the relaxor ferroelectrics family, receiving special attention for its technical importance [20]. However, its preparation usually needs the addition of $BaTiO_3$ (BT) and $PbTiO_3$ (PT) to obtain pure phases [16,21].

On the other hand, a considerable number of compositions from the Aurivillius family exhibit a relaxor ferroelectric behaviour [22-26]. The Aurivillius compounds are layered bismuth $[Bi_2O_2]^{2+}[A_{n-1}B_nO_{3n+1}]^{2-}$, where the sites A and B can be occupied for different elements. These are formed by the regular stacking of Bi_2O_2 slabs and perovskite-like blocks $A_{n-1}B_nO_{3n+1}$. These materials have received great attention due to their large remanent polarization, lead-free nature, relatively low processing temperatures, high Curie temperatures and excellent piezoelectric properties, which made them good candidates for high-temperature piezoelectric applications and memory storage [27]. The origin of the relaxor behaviour for these materials have been associated to a positional disorder of cations on A or B sites of the perovskite blocks that delay the evolution of long-rage polar ordering [28].

Several models have been proposed to explain the dielectric behaviour of relaxor ferroelectrics. The basic ideas have been related to the dynamics and formation of the polar nanoregions (PNRs). In this way, Smolenskii proposed the existence of compositional fluctuations on the nanometer scale taking into account a statistical distribution for the phase transition temperature [29]. On the other hand, Cross extended the Smolenskii's theory to a superparaelectric model associating the relaxor behaviour to a thermally activated ensemble of superparaelectric clusters [30]. Viehland et al. have showed that cooperative interactions among these superparaelectric clusters could produce a glass-like freezing behaviour, commonly exhibited in spin-glass systems [31]. Later, Qian and Bursill [32] analyzed the possible influence of random electric fields on the formation and dynamics of the polar clusters, which can be originated from nano-scaled chemical defects. They have also proposed that the relaxor behaviour can be associated to a dipolar moment in an anisotropic double-well potential, taking into account only two characteristic relaxation times. According to this model, the dispersive behaviour is produced by changes in the clusters size and the correlation length (defined as the distance, above which such PNRs become non-interactive regions) as a function of the temperature, which provides a distribution function for the activation energy. However, despite their very attractive physical properties, the identification of the nature of the dielectric response in relaxors systems still remains open and requires additional theoretical and experimental information, which can be very interesting to contribute to the explanation of the origin of the observed anomalies.

The present chapter shows the studies carried out on several relaxor ferroelectric ceramic materials, which have been developed by the present authors. Lanthanum modified lead zirconatetitanate ceramics will be evaluated considering different La^{3+} concentrations and Zr/Ti ratios. It will be discussed the dynamical behaviour of the PNRs taking into account a relaxation model, which considers a distribution function for the relaxation times. The influence of A or B vacancies on the relaxor behaviour will be also analyzed considering the decoupling effects of these defects in the Pb-O-Ti/Zr bounding. For the PZN-PT-BT system, the relaxor behaviour will be explained considering the presence of local compositional fluctuation on a macroscopic scale. Finally, the relaxor behaviour of $Sr_{0.50}Ba_{0.50}Bi_2Nb_2O_9$ ferroelectric ceramics, which belong to the Aurivillius family, will be discussed considering a positional disorder of cations on A or B sites of the perovskite blocks.

2. Lanthanum modified Lead Zirconate Titanate (PLZT)

2.1. Relaxor behaviour and coexistence of AFE and FE phases

Several researches concerning PZT properties have shown that very good properties can be obtained by suitable selection of the Zr/Ti ratio and the substitution of a small amount of isovalent or heterovalent elements for the Pb or (Zr,Ti) sublattices [1]. Especial attention receives the Zr-rich PZT-type ceramics, which exhibit interesting dielectric and pyroelectric characteristics, suitable for pyroelectric detectors, energy converters, imaging systems, etc [1,33-34]. They show orthorhombic antiferroelectric (AFE-O), low temperature rhombohedral ferroelectric (FR-LT), high temperature rhombohedral ferroelectric (FR-HT) and cubic paraelectric (PC) phase sequence [1].

One of the most common additives to the PZT ceramics is the lanthanum cation, which substitute the Pb-ions in the A-site of the perovskite structure [1]. The lanthanum-modified lead zirconatetitanate $Pb_{1-x}La_x(Zr_{1-y}Ti_y)_{1-x/4}O_3$ (PLZT) ferroelectric ceramics show excellent properties to be considered for practical applications, especially PLZT x/65/35, x/70/30 and x/80/20 compositions due to the relaxor ferroelectric behaviour [35-36]. For Zr-rich PZT ceramics, which are close to the antiferroelectric-ferroelectric (AFE-FE) phase boundary, the FE phase is only marginally stable over the AFE [33]. In this way, as the FE state is disrupted by lanthanum modification, the AFE state is stabilized [33].
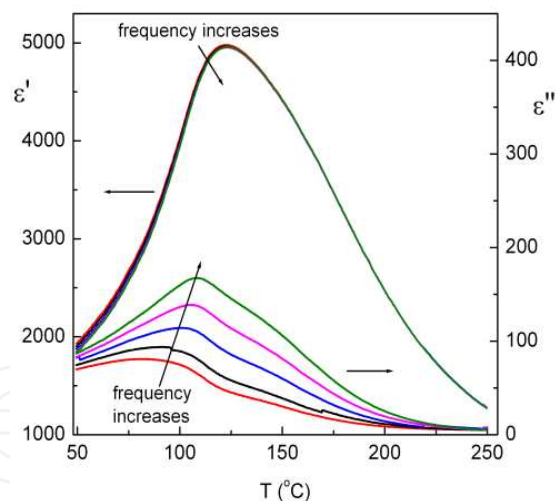

Figure 1. Temperature dependence of the real (ε') and imaginary (ε'') parts of the dielectric permittivity at several frequencies for PLZT 6/80/20 ferroelectric ceramic system.

Figure 1 shows the temperature dependence of the real (ε') and imaginary (ε'') parts of the dielectric permittivity, at several frequencies, for PLZT 6/80/20 ferroelectric ceramic system. Typical characteristics of relaxor ferroelectric behaviour are observed. The frequency dependence of ε' is very weak but the frequency dependence of ε'' clearly reflects the relaxor nature of the system. The asymmetrical shape of the curves could suggest the existence of more than one contribution. X-ray diffraction analysis for the PLZT 6/80/20 ceramic samples

have previously shown a mixture of FE and AFE phases at room temperature [13]. Polarized light microscopy studies were performed on the ceramic system in a wide temperature range. Aggregates of individual regions were observed, which were associated to FE and AFE phases. As the temperature increased, a gradual change was observed, suggesting a transition to a single phase [13].

Figure 2 shows the hysteresis loops obtained for the PLZT 6/80/20 ceramics for two temperatures, as example of the obtained behaviour in a wide temperature range. Around 70°C a double-loop-like behaviour was observed suggesting an induced FE-AFE transformation.The FE state is disrupted by the lanthanum modification and the AFE state is stabilized, which may be a consequence of the short-range nature of the interaction between the AFE sublattices. The double-loop remains for higher temperature and around 120°C the loop disappears suggesting a transition to a PE phase. Then, it is possible to consider the coexistence of two phase transitions: a FE-AFE phase transition observed around 70°C and an AFE-PE phase transition around 120°C. Note, that the maximum of ε' is observed around 120°C. Negative values for T_C were found, which has confirmed that around 120°C an AFE-PE transition take places [13]. Thus, the relaxor ferroelectric behaviour for this system could be associated to the coexistence of FE and AFE phases in the studied material.
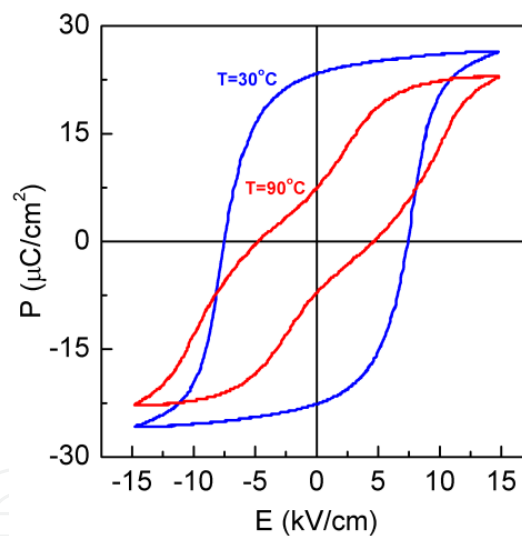

Figure 2. Hysteresis loops for PLZT 6/80/20 ferroelectric ceramic system.

2.2. A relaxation model

The nature of the relaxor behaviour is determined by the existence of PNRs, which possess different relaxation times [32,37]. The relaxation time (τ) represents the time response of such PNRs or polarization mechanisms to change with the applied electric field. However, this process does not occur instantaneously. Indeed, there exists certain inertia, which is the cause of the pronounced dielectric relaxation in relaxor ferroelectrics. The polar nanoregions appear below a certain temperature, the so-called the Burns' temperature (T_B) [38], which is

typically hundreds degrees above the temperature of the maximum real dielectric permittivity (T_m). On cooling, the number, size (some of them) and the interaction of the PNRs increase [39]. The increase of such interactions promotes the freezing of some regions around certain temperatures below T_m, known as the freezing temperature (T_F). Two fundamental polarization mechanisms have been reported, which have been associated with the dynamics of the PNRs; (i) dipole reorientation [37,40] and (ii) domain wall vibrations [32]. Both mechanisms have a characteristic time response, which depends on the temperature and size of the PNRs. If the contributions of an ensemble of these regions are considered, the macroscopic polarization function, at fixed temperature, can be expressed by [41]:

$$P(t) = P_{01}e^{-\frac{t}{\tau_1}} + P_{02}e^{-\frac{t}{\tau_2}} + P_{03}e^{-\frac{t}{\tau_3}} + ... = \sum_i P_{0i}e^{-\frac{t}{\tau_i}} \tag{1}$$

where τ_i is the relaxation time of the ith PNR and P_{0i} takes the form of equation (2), in analogy with the Debye single relaxation time model, which takes into account a distribution function of relaxation times [41]:

$$P_{0i} = \frac{\varepsilon_s - \varepsilon_\infty}{\tau_i} g(\tau_i) \tag{2}$$

$$g(\tau_i) = \frac{2\sigma}{\pi} \frac{1}{4(\ln\frac{\tau_i}{\tau_0})^2 + \sigma^2} \tag{3}$$

In these relations $g(\tau_i)$ is a distribution function for the logarithms of the relaxation times, which has been assumed to be a Lorentz rather than a Gaussian distribution function; τ_0 and σ are the mean relaxation time and the Standard Deviation, respectively. According to the Debye model, the frequency dependence of the complex dielectric permittivity can be expressed as:

$$\varepsilon*(\omega) = \varepsilon' - i\varepsilon'' = \varepsilon_\infty + \int P(t)e^{-i\omega t}dt \tag{4}$$

where ε_s and ε_∞ are the low (static) and high (optical) dielectric permittivity, respectively, ω the measurement frequency, and P(t) the decay polarization function. Substituting equations (1), (2) and (3) into equation (4), the real and imaginary component of the dielectric permittivity for the multi-relaxation times approximation can be obtained and expressed as in equations (5) and (6). It is important to point out that equations (5) and (6) have been de-

rived from the discrete expression (1), taking into account the values of the relaxation times (τ_i) close to each other [41].

$$\varepsilon'(\omega,T) = \varepsilon_\infty + (\varepsilon_s - \varepsilon_\infty)\frac{2\sigma}{\pi}\int_{-\infty}^{+\infty}\frac{1}{(4z^2+\sigma^2)(1+\omega^2\tau_0^2\exp(2z))}dz \qquad (5)$$

$$\varepsilon''(\omega,T) = (\varepsilon_s - \varepsilon_\infty)\frac{2\sigma}{\pi}\int_{-\infty}^{+\infty}\frac{\omega\tau_0\exp(z)}{(4z^2+\sigma^2)(1+\omega^2\tau_0^2\exp(2z))}dz \qquad (6)$$

It has been considered in equations (5) and (6) that $z = \ln\tau/\tau_0$. By using the experimental results of $\varepsilon'(\omega,T)$ and $\varepsilon''(\omega,T)$ for two frequencies, the temperature dependence of dielectric parameters, such as, τ_0, ε_s and σ can be obtained as a solution of the equations system. After that, by using the theoretical results of $\tau_0(T)$, $\varepsilon_s(T)$ and $\sigma(T)$, the theoretical dependences of $\varepsilon'(\omega,T)$ and $\varepsilon''(\omega,T)$ can be obtained for the studied frequency and temperature ranges. The parameter ε_∞ has been considered negligible because of the high values of the dielectric permittivity in ferroelectric systems [1].

Figures 3 and 4 show the temperature dependence of the real (ε') and imaginary (ε'') components of the dielectric permittivity (symbols), at several frequencies, for the studied PLZT 10/80/20 composition. A relaxor characteristic behaviour can be observed. The maximum real dielectric permittivity decreases, while its corresponding temperature (T_m) increases, with the increase of the measurement frequency. There is not any peak for ε'' due to the low temperature range where the maximum of the real part of the dielectric permittivity appears, i.e. the maximum for ε'' should appear below the room temperature.
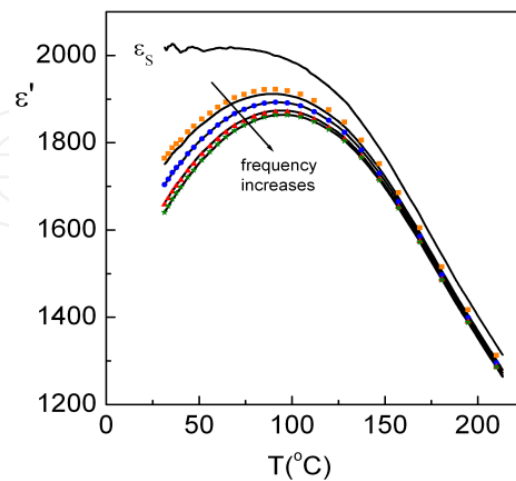

Figure 3. Temperature dependence of the real part (ε') of the dielectric permittivity at several frequencies for PLZT 10/80/20 ferroelectric ceramic system. The experimental values are represented by solid points and the theoretical results by solid lines. It has been included the theoretical temperature dependence of the static dielectric permittivity (ε_s).
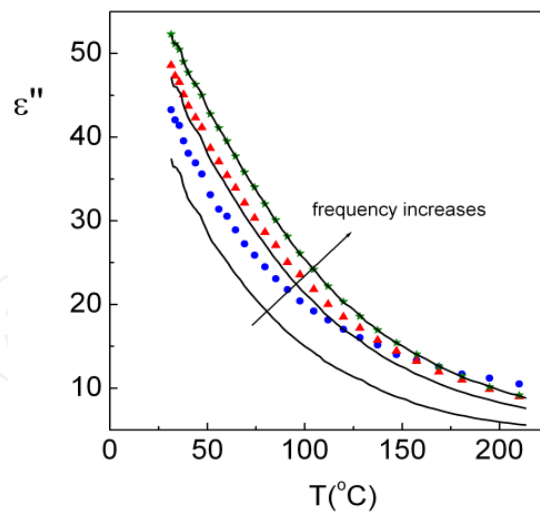
Figure 4. Temperature dependence of the imaginary part (ε'') of the dielectric permittivity at several frequencies for PLZT 10/80/20 ferroelectric ceramic system. The experimental values are represented by solid points and the theoretical results by solid lines.

The number of PNRs able to follow the applied external electric field switching decreases with the increase of the frequency, so that only such inertial-less regions contribute to the dielectric permittivity (those regions whose activation energy is close to thermal energy k_BT, being k_B the Boltzmann constant). Therefore, due to the cooperative nature, the real component of the dielectric permittivity should decrease with the increase of the measurement frequency.

The maximum for ε' in relaxor systems is not related to a crystallographic transition. Indeed, such a maximum corresponds to rapid changes of the fraction of the frozen Polar Regions [39]. Hence, the shift up to higher temperatures of the maximum for ε' with the increase of the frequency is a direct consequence of the delay in dielectric response of the frozen regions.

By using equations (5) and (6) and the experimental data of Figures 3 and 4, the temperature dependences of ε_s, σ and τ_0 were obtained. The results were obtained by numerical methods because there was no analytical solution for the equation system. The theoretical curves for ε' and ε'' were obtained for all the studied frequency range, and shown in the same Figures 3 and 4 as solid lines, for the studied system. The temperature dependence of the static dielectric permittivity (ε_s) is also shown in Figure 3. A good agreement between experimental and theoretical results can be observed. It is important to point out that the deviation between the experimental and theoretical results, observed at low frequencies for the temperature dependence of ε'', can be associated with the contribution of the electric conductivity to the dielectric response, which has not been considered in the proposed model.

Figure 5 shows the temperature dependence of $\ln\tau_0$ and σ for the studied composition. As can be seen, $\ln\tau_0$ increases with the increase of the temperature, passes through a maximum and then decreases for higher temperatures. Similar results have been previously reported by Lin et al [41]. According to the model, the logarithmic mean relaxation time ($\ln\tau_0$) should have has approximately the same tendency as that of $\sigma(T)$. Both parameters increases when

the temperature decreases which can be understood as a consequence of the increased iner-
tia of the dipolar clusters as they become more correlated with each other upon cooling. This
observation also could reflect a dynamic change in the well potential for the shifting ions.
However, the reduction in $\ln\tau_0(T)$ at lower temperatures possibly could reflect a freezing
phenomenon of some clusters that are saturated in correlation, which leads to the frustration
of cooperative interactions and, hence, leaves only relatively unstrained or smaller clusters
available to couple with the electric field. Also, one could speculate that such clusters are the
regions within the domain boundaries between the frozen regions.
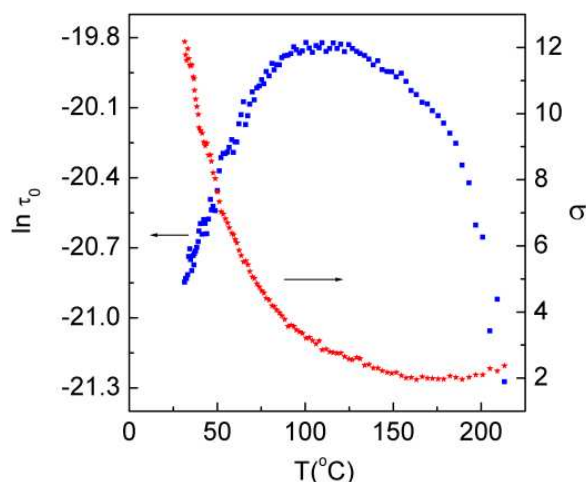
Figure 5. Temperature dependence of the main relaxation time (logarithmic representation, $\ln\tau_0$) and its standard de-
viation (σ), for PLZT 10/80/20 ferroelectric ceramic system.

In this way, the size and the interaction between PNRs increase on cooling from the high
temperature region and its contribution to the dielectric permittivity becomes negligible be-
low the freezing temperature (T_F) [39]. In this temperature range ($T < T_F$), the applied electric
field is not strong enough to break such interactions and only the smallest regions can
switch with the electric field, i.e. that is to say, there is a frustration of the cooperative effect.
For temperatures above T_F, there are fluctuations between equivalent polarization states
[30], leading to a decrease of the macroscopic polarization upon heating [42]. The applied
electric field cannot reorient the ferroelectric dipoles because of the thermal fluctuation. The
potential barrier between equivalent polarization states decreases with the increase of the
temperature and the thermal energy promotes the spontaneous switching of the dipoles,
even when an electric field is applied. The contribution to the dielectric permittivity is due
to those PNRs, which can switch with the applied electric field. Thus, for temperatures
slightly above T_F all the PNRs could contribute to the dielectric permittivity and a maximum
value of the mean relaxation time could be expected. Therefore, the temperature corre-
sponding to the maximum of $\ln\tau_0$ can be related to the freezing temperature. The standard
deviation (σ), which can be interpreted as the correlation between the PNRs [32,41], decreas-
es upon heating and it is relatively small at high temperatures. When the temperature in-
creases the thermal energy is high enough to break down the interaction between the PNRs.

So that, a decrement of the correlation between the PNRs is promoted by an increase of the temperature and the Standard deviation decreases up to a relatively constant value around the Burns' temperature (T_B) [38,43], where the PNRs completely disappear.
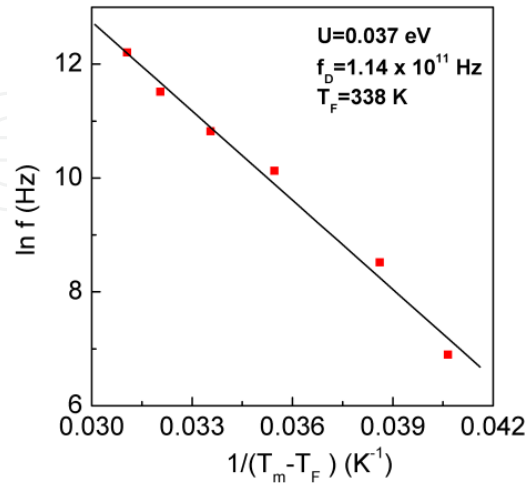

Figure 6. Temperature dependence of the frequency (lnf versus $1/(T_m-T_F)$ curve) for PLZT 10/80/20 ferroelectric ceramic system. Solid lines represent the fitting by using the Vogel–Fulcher relation.

The freezing temperature (T_F) was determined by using the Vogel–Fulcher relation [44], as expressed by equation (7):

$$f = f_D e^{-\frac{U}{k_B(T_m - T_F)}} \qquad (7)$$

where f_D is the Debye frequency and U is the activation energy. Figure 6 show the temperature dependence of the frequency (lnf versus $1/(T_m-T_F)$ curve) and the fitting by using equation (7). In order to maintain the standard representation, the temperature in Figure 6 was expressed in Kelvin. The fitting parameters U, f_D and T_F have been included in the figure. The results are in agreement with previously reported results in the literature [42]. The disagreement between the T_F value, which has been determined by using the Vogel-Fulcherrelation, and the temperature corresponding to the maximum value of $\ln\tau_0$ could be associated to the diffusivity of the phase transition in the studied system.

2.3. Relaxor behaviour and vacancies.

Relaxor ferroelectrics are formed by temperature dependent Polar Nanometric Regions (PNRs), which possess different volumes [45] and orientations for the polarization [30,37,46-47]. The PNRs appear at elevated temperatures (in the paraelectric state), at the so-called Burns' temperature (T_B) [38,48-49], due to short-range interactions, which establish a local polarization thermally fluctuating between equivalents polar states.

The disorder in the arrangement of different ions on the crystallographic equivalent sites is the common feature of relaxors [50]. This is associated, in general, with a complex perovskite of the type $A(B'B'')O_3$, where the B sites of the structure are occupied by different cations. Nevertheless, in lead zirconate titanate based ceramics (PZT) the disorder due to the arrangement of the isovalent cations Zr^{4+} and Ti^{4+}, in the B site of the structure, does not lead to relaxor behaviour for any Zr/Ti ratio. The lanthanum modification on this system, above certain La^{3+} concentrations, provides a relaxor ferroelectric state [11-12]. Electrical neutrality can be achieved, stoichiometrically, considering the vacancies formation either in the A-site (Pb^{2+}) or in the B-site (Zr^{4+}, Ti^{4+}), or on both. The distortion of the crystalline lattice in the PZT system could promote the formation of the PNRs. In this section, the results concerning the influence of the A or B vacancies defects in the relaxor ferroelectric behaviour of lanthanum modified PZT ceramic samples will be presented. The studied compositions will be $Pb_{0.85}La_{0.10}(Zr_{0.60}Ti_{0.40})O_3$ and $Pb_{0.90}La_{0.10}(Zr_{0.60}Ti_{0.40})_{0.975}O_3$, labelled as PLZT10-VA and PLZT10-VB, respectively.

The temperature dependence of the real dielectric permittivity (ε') and the dielectric losses (tan δ) are shown in the Figures 7 and 8, respectively, for several frequencies. Typical characteristics of relaxor ferroelectrics are exhibited for both samples, i.e. wide peaks for ε', the maximum real dielectric permittivity shifts to higher temperatures with the increase of the frequency, and the maximum dielectric losses temperature appears at temperatures below T_m. On the other hand, it can be observed that the dielectric response is highly affected by the type of compensation. The maximum values of the real dielectric permittivity in the PLZT10-VA sample are lower than those obtained for the PLZT-10VB sample, and appear at lower temperatures. The PLZT10-VA sample also exhibits a larger temperature shift of T_m ($\Delta T=15^oC$), from 1 kHz to 1 MHz, than that of the PLZT10-VB sample ($\Delta T=9^oC$).
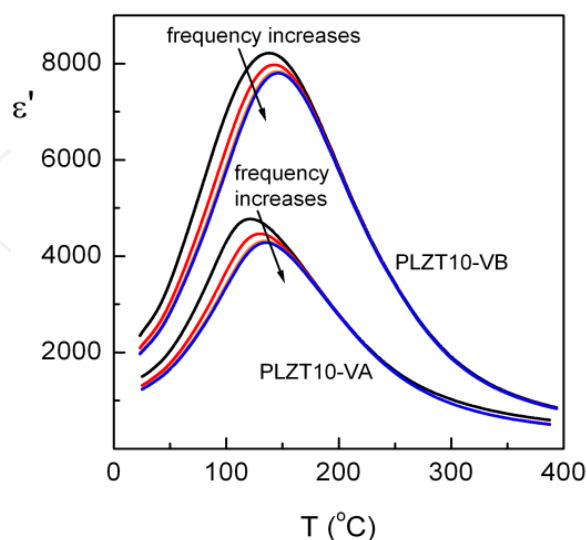

Figure 7. Temperature dependence of the real (ε') component of the dielectric permittivity at several frequencies, for PLZT10-VA and PLZT10-VB ceramic samples.

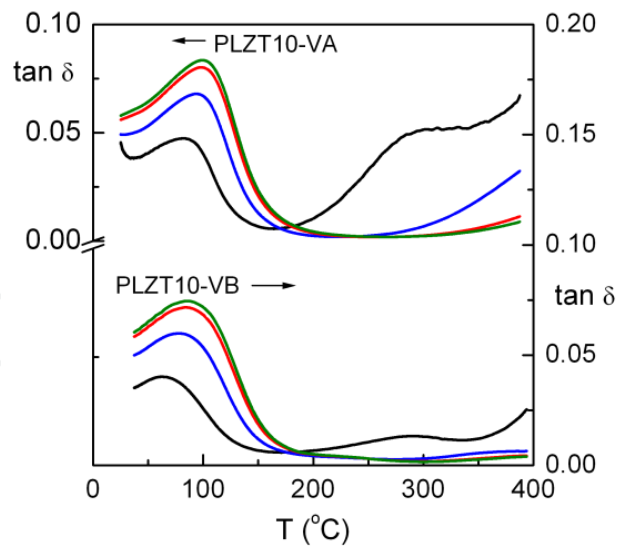**Figure 8.** Temperature dependence of the dielectric losses (tan δ) at several frequencies for PLZT10-VA and PLZT10-VB ceramic systems.

It has been previously commented that, in relaxors, the maximum real dielectric permittivity is not a consequence of crystallographic changes but it is associated with a rapid change in the volume fraction of frozen polar nanoregions [39]. During cooling, the PNRs grow in size and number [39,43] as well as the interactions among them increases. Thus, a decrement of its mobility is expected; the thermal energy (k_BT) is not enough to switch the polar state of the PNRs (freezing phenomenon). While the regions grow, with the decreasing of the temperature, the thermal energy k_BT decreases. The freezing process begins at high temperatures and finish at low temperatures, below T_m, in the so called freezing temperature (T_F), where all the PNRs are frozen.

The dielectric and ferroelectric response in relaxor ferroelectrics strongly depend of the temperature dependence of the freezing process (dynamic of the PNRs) as well as on the interactions between external electric field and the dipole moment of the PNRs. When a weak alternating electric field is applied, only the unfrozen regions and the frozen ones with activation energies close to k_BT could switch with the applied alternating electric field. Therefore, only these regions contribute to the dielectric permittivity. However, not all these regions can switch at any excitation frequency; the number of PNRs able to follow the applied external electric field switching decreases with the increase of the frequency [14]. The response also depends on the relaxation time of each region [14, 41]. Thus, the dielectric response in relaxors depends of the number of regions that can contribute at each temperature and the distribution of the corresponding relaxation times.

The Pb^{2+} ions (*A*-sites of the perovskite structure) establish the long-range order in PZT based ceramics due to strong coupling of Pb-O-Ti/Zr bonding [51]. The coupling defines the height of the energy barrier between polar states via Ti/Zr-hopping [51]. The Pb^{2+} substitution by La^{3+} ions, above certain level of La^{3+} ions concentration, weakens this bonding resulting in small and broadly distributed energy barriers [51], which disrupts the long-range

order and promotes the PNRs formations. An additional contribution, which plays a fundamental role in the relaxor behaviour, can be originated from the *A*- or *B*-sites vacancies formations. There are two important differences between the *A*- or *B*-site compensation, which can explain the different dielectric behaviour observed in the studied samples: *i*) for the same lanthanum concentration the number of lead vacancies is twice the Zr/Ti vacancies, if it is considered *A*- or *B*-site compensation, respectively, i.e. $2La^{3+} \rightarrow 1V_{Pb}$ and $4La^{3+} \rightarrow 1V_{Zr/Ti}$; *ii*) the *A*-site vacancies generate large inhomogeneous electric fields, which reduce the barriers between energy minima for different polarization directions [20], and promote the decoupling of the Pb-O-Ti/Zr bonding, making the corresponding Ti/Zr-hopping easier due to the lack of lead ions. For the case of the *B*-site vacancies, all the Ti/Zr ions are well coupled to the lead or the lanthanum ions.

From this point of view, it could be pointed out that for the PLZT10-VA sample the defects concentration, which could promote the PNRs formation, is higher than that for the PLZT10-VB sample. On the other hand, the thermal energy, which could change the nanoregions polarization state, is smaller for the PLZT10-VA sample as a consequence of the smaller hopping barrier. Considering these analyses, it could be explained the lower T_m values of the real part of the dielectric permittivity for the PLZT10-VA. The observed results are in agreement with previous reports for lead based systems with and without Pb^{2+} vacancies [52].

The larger temperature shift of T_m, which was analyzed for the PLZT10-VA, could be related to a higher temperature dependence of the freezing process around T_m, i.e. higher temperature dependence in the change of the volume fraction of frozen polar nanoregions around T_m. The number of PNRs, which can follow the electric field switching, decreases with the increase of the frequency. Thus, the maximum value of ε' decreases when the frequency increases, and also shifts to higher temperatures.

From the Figure 8, it is observed that the maximum values of the dielectric losses, for both samples, are observed in the same temperature range. No remarkable differences exist as can be expected from the difference observed in the T_m values between both systems. This could suggest similar dipolar dynamic in the temperature range for both ceramics.

Figure 9 shows the temperature dependence of the remanent polarization (P_R) for both samples. The PLZT10-VB sample exhibits higher values, which is in agreement with the previous discussion concerning the hopping barrier. The decoupling introduced by *A*-site vacancies affects the total dipolar moment of the system and, consequently, the macroscopic polarization is affected. Thus, the magnitude of the polarization decreases with the increase of the *A*-site vacancies concentration.

On the other hand, the remanent polarization for both samples shows an anomaly in the same temperature region (70–85°C), which could be associated with the 'offset' of the freezing process [14, 53]. This result suggests that the freezing temperature (T_F) could be the same for both samples or, at less the dynamic of PNRs is the same in both systems for that temperature range. Furthermore, the anomaly is observed in the same region where the maximum values of the dielectric losses have been observed, which could suggest a relation between the freezing phenomenon and the temperature evolution of dielectric losses.
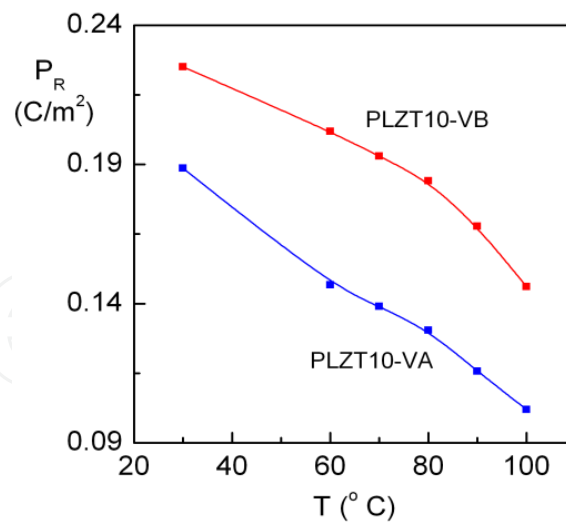
Figure 9. Temperature dependence of remnant polarization for the PLZT10-VA and PLZT10-VB samples. The lines between dots are only a guide to the eyes.

3. Other typical relaxor ferroelectric perovskites

Relaxor-based ferroelectric materials $PbMg_{1/3}Nb_{2/3}O_3$–$PbTiO_3$ (PMN–PT) and $PbZn_{1/3}Nb_{2/3}O_3$–$PbTiO_3$ (PZN–PT) have been extensively studied due to their high electromechanical coupling factor and piezoelectric coefficient [3,8,16-21,43-44,54-57].

It is known that the large dielectric permittivity of perovskite relaxor ferroelectrics, such as $(PbMg_{1/3}Nb_{2/3}O_3)_{1-x}(PbTiO_3)_x$, comes from ferroelectric like polar nanoregions [30]. Upon lowering the temperature these nanoregions grow slightly [43] but do not form long-range ferroelectric order. The temperature dependence of the dielectric permittivity shows a frequency-dependent peak as the polar nanoregion orientations undergo some sort of glassy kinetic freezing. Analyses of the phase and microstructure evolution for these materials have showed that the increase in the sintering temperature caused the weakening of the dielectric relaxor behaviour [54]. It has been related to compositional fluctuation and the release of the internal stresses, leading to the decrease in the short-range *B*-site order.

The PNRs freezing process in $PbMg_{1/3}Nb_{2/3}O_3$ has been analyzed considering both polarization and strain operating on subtly different timescales and length scales [57]. The strain fields are considered as relatively weak but longer ranging, while the dipole interactions tend to be short range and relatively strong. It has been discussed that the elastic shear strain fields is partly suppressed by cation disordering and screened by the presence of antiphase boundaries with their own distinctive strain and elastic properties, which provide a mechanism for suppressing longer ranging correlations of strain fields.

On the other hand, the barium modified PZN-PT system has shown excellent piezoelectric properties [58]. The preparation of PZN system usually needs the addition of $BaTiO_3$ (BT) to obtain pure phases. Therefore, the ternary system PZN-PT-BT has received wider attention,

showing high values of the dielectric permittivity and the pyroelectric coefficient [21,59]. This material shows lower diffuseness of the phase transition and weaker frequency dispersion of the dielectric response than that of the PZN-BT system [16]. It has been shown that it could be interesting try to decrease the transition temperature and to grow the value of the figure of merit in order to obtain better materials for practical applications [17-18,21,60-61].

The present authors have developed several researches concerning $(Pb_{0.8}Ba_{0.2})$ $[(Zn_{1/3}Nb_{2/3})_{0.7}Ti_{0.3}]O_3$ (PZN-PT-BT) system [19,62-63]. A Positive Temperature Coefficient of Resistivity (PTCR) effect has been studied. This effect has found extensive applications as thermal fuses, thermistors, safety circuits and other overload protection devices [64]. It has been discussed that the PTCR behaviour primarily arise from the Schottky barrier formed at grain boundary regions, which act as effective electron traps of the available electrons from the oxygen vacancies in the ceramic, increasing the Schottky barrier height of the material. Excellent properties to be used in dielectric and pyroelectric applications have been also reported [63].

Figure 10 shows the temperature dependence of the real part (ε') of the dielectric permittivity for the $(Pb_{0.8}Ba_{0.2})[(Zn_{1/3}Nb_{2/3})_{0.7}Ti_{0.3}]O_3$ ferroelectric ceramic system at several frequencies. Typical characteristics of relaxor ferroelectrics are observed. There is a strong dispersion of the maximum of ε' and its corresponding temperature shift towards higher temperatures when the frequency increases. On the other hand, the system did not follow a Curie–Weiss–like behaviour above T_m. For relaxor ferroelectrics, some of the dipoles are frozen during the time scale of measurement. The fraction of frozen dipoles in itself is a function of the temperature, so Curie-Weiss's law is no longer valid.
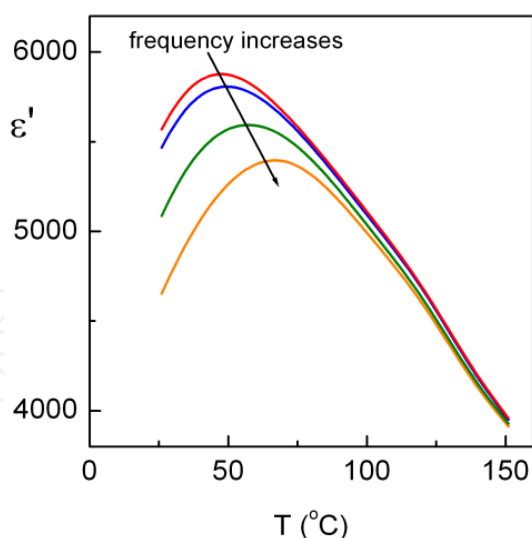

Figure 10. Temperature dependence of the real (ε') part of the dielectric permittivity at several frequencies for $(Pb_{0.8}Ba_{0.2})[(Zn_{1/3}Nb_{2/3})_{0.7}Ti_{0.3}]O_3$ ferroelectric ceramic system.

For $Pb(B'_{1/3}B''_{2/3})O_3$ type pervoskites, it has been reported a particular microstructure where the B-site 1:1 short-range-ordered nanodomains (rich in B' ions) are embedded in a matrix rich in B'' ions, which promotes a compositional inhomogeneity [65]. The nonstoichiometric

ordering induces strong charge effects; i.e., the ordered domains have a negative charge with respect to the disordered matrix. Thus, the charge imbalance inhibits the growth of domains and nanodomains are obtained in a disordered matrix with polar micro-regions.
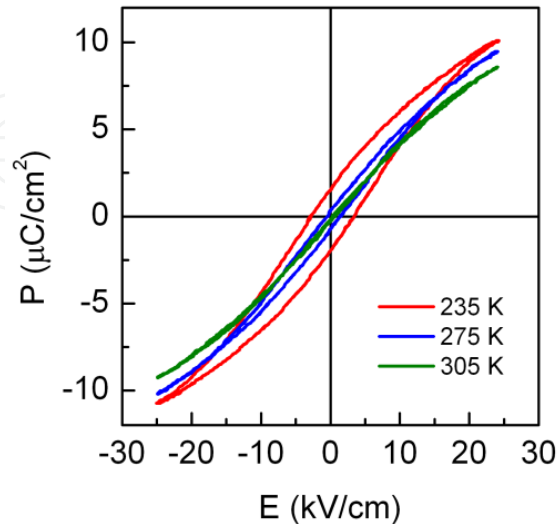

Figure 11. Hysteresis loops for $(Pb_{0.8}Ba_{0.2})[(Zn_{1/3}Nb_{2/3})_{0.7}Ti_{0.3}]O_3$ ferroelectric ceramic system.

Figure 11 shows the hysteresis loops at several temperatures for the studied system. Slim P-E loops and small remanent polarization values are observed. The slim-loop nature suggests that most of the aligned dipole moments switch back to a randomly oriented state upon removal of the field. It could be interpreted in terms of correlated polar nanodomains embedded in a paraelectric matrix [44]. For relaxor ferroelectric materials, there is a micro- to macro-domain transition [66]. In the absence of any external field, the domain structure of relaxor ferroelectrics contains randomly oriented micropolar regions. When an electric field is applied, the micro-domains are oriented along the field direction and the macro-domains appear. The micro- to macro-domain transition has been confirmed by 'in-situ' switching by means of an electron beam inducing local stresses to align the domains [66].

4. Lead free Aurivillius relaxor ferroelectrics

The temperature dependence of the real (ε') and imaginary (ε'') parts of the dielectric permittivity, at several frequencies, for the $Sr_{0.5}Ba_{0.5}Bi_2Nb_2O_9$ sample are showed in the Figure 12. The maximum of ε' decreases with the increase of the frequency; its corresponding temperature (T_m) shifts with the frequency, showing a high frequency dispersion. For the imaginary part (ε'') the maximum values are observed at lower temperatures than those the observed for ε' and the corresponding temperature again shows a significant frequency dispersion. These characteristics are typical of relaxor ferroelectric materials. On the other hand, an abrupt increase of ε'' is observed in the higher temperature zone, which is more clear in the low frequency range. This behaviour could be associated to the conductivity losses.
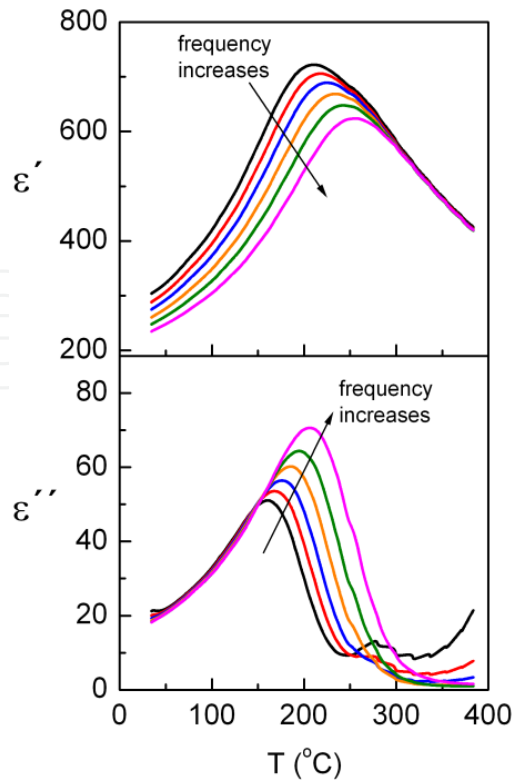
Figure 12. Temperature dependence of the real (ε') and imaginary (ε'') parts of the dielectric permittivity, at several frequencies, for the $Sr_{0.5}Ba_{0.5}Bi_2Nb_2O_9$.

The origin of the relaxor behaviour for this material can be explained from a positional disorder of cations on *A* or *B* sites of the perovskite blocks that delay the evolution of long-range polar ordering [28]. Previous studies in the $SrBi_2Nb_2O_9$ system have showed that the incorporation of barium to this system conduces to a relaxor behaviour in the ferroelectric-paraelectric phase transition [28,67] and the increases of barium content enhance the degree of the frequency dispersion of the dielectric parameters [67]. This behaviour can be explained considering that the barium ions can substitute the strontium ions in the *A* site of the perovskite block but enter in the $Bi_2O_2^{2+}$ layers, conducting to an inhomogeneous distribution of barium and local charge imbalance in the layered structure. The incorporation of barium ions to bismuth sites takes care to reduce the constrain existent between the perovskite blocks and the layered structure [68].

The relaxor behaviour is usually characterized by using the variation of T_m with frequency (ΔT), degree of the frequency dispersion, and the critical exponent (δ) obtained from the following law [67]:

$$\frac{1}{\varepsilon'} - \frac{1}{\varepsilon'_{max}} = \frac{\left(T - T_m\right)^{\delta}}{C} \tag{8}$$

where ε'_{max} is the maximum value for the real part of the dielectric permittivity, and δ and C are constants. For an ideal relaxor ferroelectric $\delta = 2$, while for a normal ferroelectric $\delta = 1$ and the system follows the Curie-Weiss law.

For the studied material, $\Delta T = 50°C$ between 1 kHz and 1 MHz, which is higher than that of the obtained values for the PMN and PLZT 8/65/35 systems [67]. Thus, the studied material shows higher frequency dispersion. However, ΔT is lower than that of the $BaBi_2Nb_2O_9$ system (BBN), which is in agreement with previous reports where ΔT decreases with the decrease of the barium concentration [67].

The Figure 13 shows the dependency of the log $(1/\varepsilon'-1/\varepsilon'_{max})$ vs. log $(T-T_m)$ at 1 MHz for the study ceramic sample. The solid points represent the experimental data and the line the fitting, which was carried out by using the equation 8. The value obtained for δ parameter is 1.71, which is in agreement with other reports for the studied system [67].
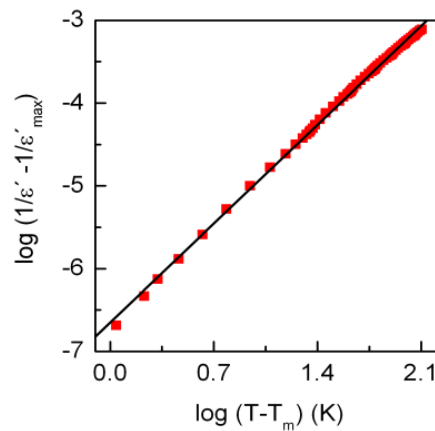

Figure 13. Dependence of the log $(1/\varepsilon'-1/\varepsilon''_{max})$ vs. log $(T-T_m)$ at 1 MHz for the $Sr_{0.5}Ba_{0.5}Bi_2Nb_2O_9$.
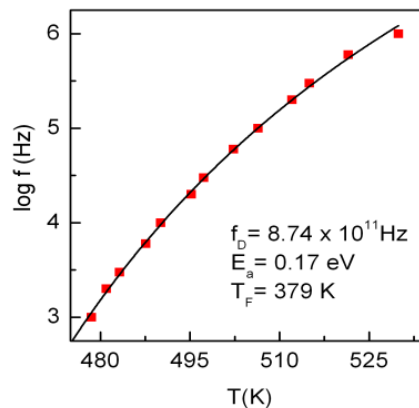
Figure 14. Dependence of the log f with T_m for the $Sr_{0.5}Ba_{0.5}Bi_2Nb_2O_9$ considering a frequency range from 1 kHz to 1 MHz. The fitting was carried out by using the Vogel-Fulcher law.

Figure 14 shows the dependence of log f with T_m for the studied material. The experimental data was fitted by using the Vogel-Fulcher law (equation 7). The fitting parameters have been included in the figure. The difference between T_m at 1 kHz and T_F is about 100 K, a higher value considering the studies carried out in PMN type relaxors [69]. On the other hand, the BBN system has showed a difference higher than 300 K, which is agreement with its strong shift of T_m [28, 69].

5. Conclusions

The relaxor behaviour has been discussed in ferroelectric perovskites-related structures. The influence of the coexistence of ferroelectric and antiferroelectric phases on the relaxor behaviour of lanthanum modified lead zirconate titanate ceramics has been analyzed. A relaxation model to evaluate the dynamical behaviour of the polar nanoregions in a relaxor ferroelectric PLZT system has been presented and the results have been discussed considering the correlation between the polar nanoregions and the freezing temperature. On the other hand, the influence of *A* or *B* vacancies on the relaxor behaviour for PLZT materials have been studied considering the decoupling effects of these defects in the Pb-O-Ti/Zr bounding and in terms of the dynamic of PNRs. Other typical relaxor ferroelectrics were analyzed too. For the PZN-PT-BT system, the relaxor behaviour was discussed considering the presence of local compositional fluctuation on a macroscopic scale. The $Sr_{0.50}Ba_{0.50}Bi_2Nb_2O_9$ ferroelectric ceramic, which is a typical relaxor from the Aurivillius family, was analyzed considering a positional disorder of cations on A or B sites of the perovskite blocks, which delay the evolution of long-rage polar ordering.

Acknowledgement

Author details

A. Peláiz-Barranco, F. Calderón-Piñar, O. García-Zaldívar and Y. González-Abreu

*Address all correspondence to: pelaiz@fisica.uh.cu

Physics Faculty–Institute of Science and Technology of Materials, Havana University, San Lázaro y L, Vedado, La Habana, Cuba

References

[1] Xu Y. Ferroelectric Materials and Their Applications. Netherland: Elsevier Science Publishers; 1991.

[2] Strukov BA., Levanyuk AP. Ferroelectric Phenomena in Crystals. Berlin: Springer-Verlag; 1998.

[3] Tai CW., Baba-Kishi KZ. Relationship between dielectric properties and structural long-range order in $(x)Pb(In_{1/2}Nb_{1/2})O_3:(1 − x)Pb(Mg_{1/3}Nb_{2/3})O_3$ relaxor ceramics. Acta Materialia 2006;54; 5631-5640.

[4] Huang S., Sun L., Feng Ch., Chen L. Relaxor behaviour of layer structured $SrBi_{1.65}La_{0.35}Nb_2O_9$. J. Appl. Phys. 2006;99; 076104.

[5] Ko JH., Kim DH., Kojima S. Correlation between the dynamics of polar nanoregions and temperature evolution of central peaks in $Pb[(Zn_{1/3}Nb_{2/3})_{0.91}Ti_{0.09}]O_3$ ferroelectric relaxors. Appl. Phys. Lett. 2007;90; 112904.

[6] Kumar P., Singh S., Juneja JK., Prakash Ch., Raina KK. Dielectric behaviour of La substituted BPZT ceramics. Physica B 2009;404(16) 2126–2129.

[7] Craciun F. Strong variation of electrostrictive coupling near an intermediate temperature of relaxor ferroelectrics. Physical Review B 2010;81; 184111.

[8] Ko JH., Kim DH., Kojima S. Low-frequency central peaks in relaxor ferroelectric PZN-9%PT single crystals. Ferroelectrics 2007; 347(1) 25-29.

[9] Samara GA. The relaxational properties of compositionally disordered ABO_3 perovskites. J. Phys.: Condens. Matter 2003;15(9) R367.

[10] Shvartsman VV., Lupascu DC. Lead-free relaxor ferroelectrics. J. Am. Ceram. Soc. 2012;95(1) 1–26.

[11] Dai X., Xu Z., Li JF., Viehland D. Effects of lanthanum modification on rombohedral $Pb(Zr_{1-x}Ti_x)O_3$ ceramics: Part I. Transformation from normal to relaxor ferroelectric behaviours. J. Mat. Res. 1996;11(3) 618-625.

[12] Dai X., Xu Z., Li JF., Viehland D. Effects of lanthanum modification on rombohedral $Pb(Zr_{1-x}Ti_x)O_3$ ceramics: Part II. Relaxor behaviour versus enhanced antiferroelectric stability. J. Mat. Res. 1996;11(3) 626-638.

[13] Peláiz-Barranco A., Mendoza ME., Calderón-Piñar F., García-Zaldívar O., López-Noda R., de los Santos-Guerra J., Eiras JA., Features on phase transitions in lanthanum-modified lead zirconate titanate ferroelectric ceramics. Sol. Sta. Comm. 2007;144(10-11) 425-428.

[14] García-Zaldívar O., Peláiz-Barranco A., Calderón-Piñar F., Fundora-Cruz A., Guerra JDS., Hall DA., Mendoza ME.. Modelling the dielectric response of lanthanum modi-

fied lead zirconate titanate ferroelectric ceramics - an approach to the phase transitions in relaxor ferroelectrics. J. Phys.: Cond. Matt. 2008;20; 445230.

[15] Peláiz Barranco A., Calderón Piñar F., Pérez Martínez O. Normal-Diffuse Transition in (Pb,La)Zr$_{0.53}$Ti$_{0.47}$O$_3$ Ferroelectric Ceramics. Phys. Sta. Sol. (b) 2000;220(1) 591-595.

[16] Fan HQ., Kong LB., Zhang LY., Yao X. Structure-property relationships in lead zinc niobate based ferroelectric ceramics. J. Appl. Phys. 1998;83; 1625-1630.

[17] Zhu WZ., Yan M., Effect of Mn-doping on the morphotropic phase boundary of PZN-BT-PT system. J. Mater. Sci. Lett. 2001;20(16) 1527-1529.

[18] Zhu WZ., Yan M., Kholkin AL., Mantas PQ., Baptista JL., Effect of tungsten doping on the dielectric response of PZN–PT–BT ceramics with the morphotropic phase boundary composition. J. Eur. Ceram. Soc. 2002;22(3) 375-381.

[19] Peláiz-Barranco A., González-Carmenate I., Calderón-Piñar F., Relaxor behaviour in PZN-PT-BT ferroelectric ceramics. Sol. Sta. Comm. 2005;134; 519-522.

[20] Haertling HG. Ferroelectric Ceramics: History and Technology. J. Am. Ceram. Soc. 1999;82(4) 797-818.

[21] Halliyal A., Kumar U., Newnham RE., Cross LE. Stabilization of the perovskite phase and dielectric properties of ceramics in the Pb(Zn$_{1/3}$Nb$_{2/3}$)O$_3$-BaTiO$_3$ system. Am. Ceram. Soc. Bull. 1987;66(4) 671-676.

[22] Jennet DB., Marchet P., El Maaoui M., Mercurio JP., From ferroelectric to relaxor behaviour in the Aurivillius-type Bi$_{4-x}$Ba$_x$Ti$_{3-x}$Nb$_x$O$_{12}$ (0<x<1.4) solid solutions. Mat. Lett. 2005;59; 376-382.

[23] Karthik C., Ravishankar N., Maglione M., Vondermuhll R., Etourneau J., Varma KBR. Relaxor behaviour of K$_{0.5}$La$_{0.5}$Bi$_2$Ta$_2$O$_9$ ceramics. Sol. Sta. Comm. 2006;139; 268–272.

[24] González-Abreu Y., Peláiz-Barranco A., Araújo EB., Franco Júnior A. Dielectric relaxation and relaxor behaviour in bi-layered perovskite. Appl. Phys. Lett. 2009;94(26) 262903.

[25] Zhang H., Yan H., Reece MJ. High temperature lead-free relaxor ferroelectric: intergrowth Aurivillius phase BaBi$_2$Nb$_2$O$_9$–Bi$_4$Ti$_3$O$_{12}$ ceramics. J. Appl. Phys. 2010;107; 104111.

[26] Chakrabarti A., Bera J. Effect of La-substitution on the structure and dielectric properties of BaBi$_4$Ti$_4$O$_{15}$ ceramics. J. Alloys Comp. 2010;505; 668–674.

[27] Rabe KM., Ahn CA. Triscone JM., editors. Physics of Ferroelectrics. Berlin Heidelberg, New York: Springer; 2007.

[28] Miranda C., Costa MEV., Avdeev M., Kholkin AL., Baptista JL., Relaxor properties of Ba-based layered perovskites. J. Eur. Ceram. Soc. 2001;21; 1303-1306.

[29] Smolienskii GA. Physical phenomena in ferroelectric with diffused phase transition. J. Phys. Soc. Japan 1970;28,Supplement; 26-30.

[30] Cross LE. Relaxor ferroelectrics. Ferroelectrics 1987;76; 241-267.

[31] Viehland D., Jang SJ., Cross LE., Wutting M. Freezing of the polarization fluctuations in lead magnesium niobate relaxors. J. Appl. Phys. 1990;68; 2916-2921.

[32] Quian H., Bursill LA., Phenomenological theory of the dielectric response of lead magnesium niobate and lead scandium tantalate. Int. J. Mod Phys. B 1996;10; 2007-2025.

[33] Ishchuk VM., Baumer VN., Sobolev VL., The influence of the coexistence of ferroelectric and antiferroelectric states on the lead lanthanum zirconate titanate crystal structure. J. Phys. Condens. Matter 2005;17(19) L177-L182.

[34] Peláiz-Barranco A., Hall DA. Influence of composition and pressure on the electric field-induced antiferroelectric to ferroelectric phase transformations in lanthanum modified lead zirconate titanate ceramics. IEEE Trans. Ultras. Ferroel. Freq. Cont. 2009;56(9) 1785-1791.

[35] Jullian Ch., Li JF., Viehland D. Comparisons of polarization switching in "hard," "soft," and relaxor ferroelectrics. J. Appl. Phys. 2005;95(8) 4316-4318.

[36] Peláiz-Barranco A., García-Zaldívar O., Calderón-Piñar F., López-Noda R., Fuentes-Betancourt J. A multi-Debye relaxation model for relaxor ferroelectrics showing diffuse phase transition. Phys. Sta. Sol. (b) 2005;242(9) 1864-1867.

[37] Bovtun V., Petzelt J., Porokhonskyy V., Kamba S., Yakimenko Y. Structure of the dielectric spectrum of relaxor ferroelectrics. J. Eur. Ceram. Soc. 2001;21(10-11) 1307-1311.

[38] Burns G., Dacol FH., Crystalline ferroelectrics with glassy polarization behaviour. Phys. Rev. B 1983;28; 2527-2530.

[39] Cheng ZY., Katiyar RS., Yao X., Bhalla AS. Temperature dependence of the dielectric constant of relaxor ferroelectrics. Phys. Rev. B 1998;57; 8166-8177.

[40] Bokov AA. Recent advances in diffuse ferroelectric phase transitions. Ferroelectrics 1992;131; 49-55.

[41] Lin HT., Van Aken DC., Huebner W. Modelling the dielectric response and relaxation spectra of relaxor ferroelectrics. J. Am. Ceram. Soc. 1999;82(10) 2698-2704.

[42] Dal-Young K., Jong-Jin Ch., Hyoun-Ee K. Birefringence study of the freezing mechanism of lanthanum-modified lead zirconate titanate relaxor ferroelectrics. J. Appl. Phys. 2003;93; 1176-1179.

[43] Xu G., Shirane G., Copley JRD., Gehring PM. Neutron elastic diffuse scattering study of $Pb(Mg_{1/3}Nb_{2/3})O_3$. Phys. Rev. B 2004;69; 064112.

[44] Viehland D., Li JF., Jang SJ., Cross LE., Wuttig M. Dipolar-glass model for lead magnesium niobate. Phys. Rev. B 1991;43; 8316-8320.

[45]   Xu G., Gehring PM., Shirane G. Coexistence and competition of local- and long-range polar orders in a ferroelectric relaxor. Phys. Rev B 2006;74; 104110.

[46]   Kirillov VV., Isupov VA. Relaxation polarization of $PbMg_{1/3}Nb_{2/3}O_3$ (PMN) a ferroelectric with a diffused phase transition. Ferroelectrics 1973;5; 3-9.

[47]   Isupov VA. Nature of physical phenomena in ferroelectric relaxors. Phys. Sol. Sta. 2003;45(6) 1107-1111.

[48]   Pirc R., Blinc R. Vogel-Fulcher freezing in relaxor ferroelectrics. Phys. Rev. B 2007;76; 020101R.

[49]   Jiménez R., Jiménez B., Carreaud J., Kiat JM., Dkhil B., Holc J., Kosec M., Algueró M. Transition between the ferroelectric and relaxor states in $0.8Pb(Mg_{1/3}Nb_{2/3})O_3$-$0.2PbTiO_3$ ceramics. Phys. Rev. B 2006;74; 184106.

[50]   Bokov AA., Ye Z-G. Recent progress in relaxor ferroelectrics with perovskite structure. J. Mat. Sci. 2006;4(1) 31-52.

[51]   Chen IW., Li P., Wang Y. Structural origin of relaxor perovskites. J. Phys. Chem. Sol. 1996;57(10); 1525-1536.

[52]   Bellaiche L., Íñiguez J., Cockayne E., Burton BP. Effects of vacancies on the properties of disordered ferroelectrics: A first-principles study. Phys. Rev. B 2007;75; 014111.

[53]   Shen M., Han J., Cao W. Electric-field-induced dielectric anomalies in C-oriented $0.955Pb\ Zn_{1/3}Nb_{2/3}O_3$-$0.045PbTiO_3$ single crystals. Appl. Phys. Lett. 2003;83(4) 731-733.

[54]   Wu N-N., Hou Y-D, Wang Ch., Zhu M-K, Song X-M, Hui Y. Effect of sintering temperature on dielectric relaxation and Raman scattering of $0.65Pb(Mg_{1/3}Nb_{2/3})O_3$–$0.35PbTiO_3$ system. J. Appl. Phys. 2009;105; 084107.

[55]   Park SE., Shrout TR. Ultrahigh strain and piezoelectric behaviour in relaxor based ferroelectric single crystals. J. Appl. Phys. 1997;82(4) 1804-1811.

[56]   Park SE., Shrout TR. Characteristics of relaxor-based piezoelectric single crystals for ultrasonic transducers. IEEE Trans. Ultrason. Ferroelectr. Freq. Control 1997;44(5) 1140-1147.

[57]   Carpenter MA., Bryson JFJ., Catalan G., Zhang SJ., Donnelly NJ. Elastic and inelastic relaxations in the relaxor ferroelectric $Pb(Mg_{1/3}Nb_{2/3})O_3$: II. Strain–order parameter coupling and dynamic softening mechanisms. J. Phys.: Condens. Matter 2012;24; 045902.

[58]   Uchino K. High electromechanical coupling piezoelectrics: relaxor and normal ferroelectric solid solutions. Sol. Sta. Ion. 1998;108(1-4) 43-52.

[59]   Deb KK., Hill MD., Roth RS., Kelly JF. Dielectric and pyroelectric properties of doped lead zinc niobate (PZN) ceramic materials. Am. Cer. Bull. 1992;71; 349-352.

[60]   Krumin A. Specific solid state features of transparent ferroelectric ceramics. Ferroelectrics 1986;69(1) 1-16.

[61] Xia F., Yao X. Piezoelectric and dielectric properties of PZN-BT-PZT solid solutions. J. Mat. Sci. 1999;34; 3341-3343.

[62] Peláiz Barranco A., González Carmenate I., Calderón Piñar F., Torres García E. AC behaviour and PTCR effect in PZN-PT-BT ferroelectric ceramics. Sol. Sta. Comm. 2004;132; 431-435.

[63] Peláiz Barranco A., Gonzalez Carmenate I., Calderón Piñar F. Dielectric and pyroelectric behaviour of $(Pb_{0.8}Ba_{0.2})[(Zn_{1/3}Nb_{2/3})_{0.7}Ti_{0.3}]O_3$ ferroelectric ceramics. Rev. Cub. Fis. 2009;26(2B) 238-241.

[64] Chang H-Yi., Liu K-S., Lin IN. Modification of PTCR behaviour of $(Sr_{0.2}Ba_{0.8})TiO_3$ materials by post-heat treatment after microwave sintering. J. Eur. Ceram. Soc. 1996;16(1) 63-70.

[65] Chen J., Chan H., Harmer MP. Ordering structure and dielectric properties of undoped and La/Na-doped $Pb(Mg_{1/3}Nb_{2/3})O_3$. J. Am. Ceram. Soc. 1989;72(4) 593-598.

[66] Randall CA., Barber DJ., Whatmore RW., Groves P. Short-range order phenomena in lead-based perovskites. Ferroelectrics 1987;76(1) 277-282.

[67] Huang S., Feng Ch., Chen L., Wang Q. Relaxor Behaviour of $Sr_{1-x}Ba_xBi_2Nb_2O_9$ Ceramics. J. Am. Ceram. Soc. 2006;89(1) 328-331.

[68] Haluska MS., Misture ST. Crystal structure refinements of the three-layer Aurivillius ceramics $Bi_2Sr_{2-x}A_xNb_2TiO_{12}$ (A=Ca,Ba, x=0,0.5,1) using combined X-ray and neutron powder diffraction. J. Solid State Chem. 2004;177; 1965-1975.

[69] Kholkin AL., Avdeev M., Costa MEV., Baptista JL. Dielectric relaxation in Ba-based layered perovskites. Appl. Phys. Letters 2001;79(5) 662-664.